

# Collision-Free Guidance Control of Small Unmanned Helicopter Using Nonlinear Model Predictive Control

Satoshi SUZUKI<sup>\*</sup>, Takahiro ISHII<sup>\*\*</sup>, Yoshihiko AIDA<sup>\*\*\*</sup>,  
Yohei FUJISAWA<sup>\*\*\*</sup>, Kojiro IZUKA<sup>\*</sup>, and Takashi KAWAMURA<sup>\*</sup>

**Abstract:** In this study, our aim is to realize collision-free guidance control for a small unmanned helicopter. The simultaneous flight of multiple small unmanned helicopters has recently attracted considerable attention for practical operation because of the high efficiency and fault tolerance capability. Collision avoidance should be considered in the guidance system of small helicopters to realize simultaneous flight. The authors adopted nonlinear model predictive control (NMPC) to design a collision-free guidance control system for small unmanned helicopters; collision avoidance was regarded as a state constraint. A hierarchical control structure consisting of an attitude control system and guidance control system was adopted to simplify the overall control system. The authors propose a simple nonlinear translational model of the helicopter to reduce the computational cost of NMPC. The effectiveness of the proposed collision-free guidance control system was verified through both numerical simulation and a flight experiment.

**Key Words:** small unmanned helicopter, collision avoidance, model predictive control.

## 1. Introduction

Unmanned aerial vehicle (UAV) technology has considerably improved in the last decade, and UAVs are now used not only in research and development but also for various practical purposes such as aerial photography, surveillance and crop dusting. UAVs are safer and more convenient than manned aircraft and can potentially have a wide range of applications. Therefore, researchers have focused on the development, operation, and autonomous control of various types of UAVs: fixed-wing-type [1],[2], helicopter-type [3]–[7], tilt-rotor-type [8], tail-sitter-type [9] and airship-type [10]. Among these, we are particularly interesting in small unmanned helicopters.

Small unmanned helicopters weighing less than 5 [kg] have recently attracted considerable attention owing to their ease of carriage and handling [11]. However, the abilities of such small helicopters are severely limited: for example, they have a small payload and short flight endurance. Moreover, small helicopters may fail frequently as a result of their limited sensing and computational payload. To overcome the problem, the simultaneous flight of multiple small unmanned helicopters has been studied [12],[13]. The main advantages of simultaneous flight are efficiency and fault tolerance. Operating efficiency may significantly increase when multiple helicopters share the same task; thus the loss of individual helicopters owing to the limited flight endurance can be compensated for. Additionally, even one helicopter has fallen into troubles, the task could be accomplished by other helicopters. Therefore, the robustness and fault tolerance capability of the entire system may be

improved. In simultaneous flight, collision is a major problem and should be taken into consideration during the design of the guidance system. Collision or obstacle avoidance is an interesting topic not only for simultaneous flight of multiple small helicopters, and there has been a great deal of theoretical and practical work done on collision/obstacle avoidance in the control, robotics, and navigation fields. Several approaches for collision avoidance for multiple mobile robots, and also for UAVs have already been proposed [14]–[26]. For example, the potential field method [14],[15], specific acceleration matching method [16], and simple geometric approach [17] are used for collision avoidance. In these methods, the potential field method is the most popular method for collision-free guidance because it can be easily implemented. However, these methods are prone to local minima. On the other hand, Model predictive control (MPC) has been adopted for collision-free guidance of UAVs in many studies [18]–[26] because the method has no local minima, and flexible design of objective function of MPC is suited for 3-dimensional guidance of UAVs. However, MPC is computationally expensive compared to other control methods. Therefore, most conventional research has been limited to theoretical works and only been verified through numerical simulation.

In this study, a collision-free guidance control system for small unmanned helicopters was designed using nonlinear model predictive control (NMPC). A hierarchical control structure and simple nonlinear guidance model of the helicopter are proposed to reduce the computational cost of NMPC. The effectiveness of the proposed guidance control system was verified by not only numerical simulation but also a flight experiment. The rest of this paper is organized as follows. The control system design for collision-free guidance control of a small unmanned helicopter is described in Section 2. The authors propose a hierarchical control structure using attitude and guidance controls; NMPC is only applied to the guidance controller to reduce the computational cost. The simulation and experi-

<sup>\*</sup> Faculty of Textile Science and Technology, Shinshu University, 3-15-1 Tokida, Ueda, Nagano 386-8567, Japan

<sup>\*\*</sup> Yamaha Motor, 2500 Shinkai, Iwata, Shizuoka 438-0025, Japan

<sup>\*\*\*</sup> Graduate School of Science and Technology, Shinshu University, 3-15-1 Tokida, Ueda, Nagano 386-8567, Japan  
E-mail: s-s-2208@shinshu-u.ac.jp

(Received October 9, 2013)

(Revised April 8, 2014)

mental results are presented in Sections 3 and 4. Finally, the conclusions are given in Section 5.

## 2. Control System Design

Figure 1 shows the overview of a small unmanned helicopter used in this study. The collision-free guidance control system for the helicopter is designed based on NMPC. In this study, a hierarchical control structure is adopted. Figure 2 shows an overview of the entire control system. The control system consists of two feedback control loops for attitude control (inner loop) and guidance control (outer loop). The attitude controller stabilizes the attitude dynamics of the helicopter and makes it follow the desired attitude. The guidance controller generates the appropriate attitude and heave command to realize the desired external force vector to guide the helicopter to the target position. NMPC was only adopted for the guidance controller; therefore, the number of states handled by NMPC and computational cost are reduced compared to the full-state feedback case. The hierarchical structure provides additional ease to the control system design. In the case of full-state feedback, it seems to be difficult to choose the weighting matrices of NMPC because the attitude dynamics of the helicopter is more complicated than translational dynamics. By contrast, the choice of the weighting matrices is straightforward when the hierarchical control structure is applied. Moreover, it is easy to apply the proposed guidance control system to other types of UAV by changing only the attitude control system. These reduced computational cost and ease of the design are main advantages of proposed control system compared with conventional control method.

In the following, the modeling of the small unmanned helicopter and design of each control system are described.

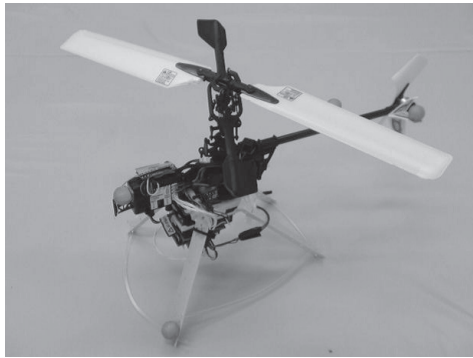


Fig. 1 Overview of small helicopter.

## 2.1 Dynamics of Small Unmanned Helicopter

The helicopter dynamics is modeled for control system design. First, the coordinate systems used for the modeling and control system design are defined.  $O$ -frame denotes the inertial frame; its origin is fixed at an arbitrary point on the ground.  $Z_O$  is aligned with the direction of gravity.  $B$ -frame denotes the body frame; its origin is fixed at the center of gravity of the helicopter.  $X_B$  is aligned with the forward direction of the body,  $Y_B$  is aligned with rightward direction, and  $Z_B$  is aligned with downward direction. The attitude of the helicopter is defined as the attitude of  $B$ -frame relative to  $O$ -frame, and the roll, pitch, and yaw angles  $\phi, \theta, \psi$  are used for attitude expression.  $C$ -frame denotes the reference frame; it has the same origin as  $B$ -frame.  $X_C$ - $Y_C$  plane is parallel with  $X_O$ - $Y_O$  plane, and this frame rotates about  $Z_O$  in conjunction with the yaw angle  $\psi$  (Fig. 3). The rotation matrix  $R_{OB}$  which expresses the rotation from  $B$ -frame to  $O$ -frame is defined by using the basis of  $B$ -frame  $x_B, y_B, z_B$  as follows:

$$R_{OB} = [x_B \ y_B \ z_B] \quad (1)$$

Similarly,  $R_{CB}$  is defined by using  $\phi, \theta, \psi$  as

$$R_{CB} = \begin{bmatrix} c_\theta c_\psi & s_\phi s_\theta c_\psi - c_\phi s_\psi & c_\phi s_\theta c_\psi + s_\phi s_\psi \\ s_\theta c_\psi & s_\phi s_\theta s_\psi + c_\phi c_\psi & c_\phi s_\theta s_\psi - s_\phi c_\psi \\ -s_\theta & s_\phi c_\theta & c_\phi c_\theta \end{bmatrix} \quad (2)$$

Here,  $c_i$  denotes  $\cos(i)$ ,  $s_i$  denotes  $\sin(i)$ , and  $i = \phi, \theta, \psi$ .

Next, the mathematical model of the small unmanned helicopter is derived. Considering the linear velocity vector of the helicopter on  $O$ -frame as  $V_O = [v_x \ v_y \ v_z]^T$ , the angular velocity of the helicopter expressed on  $B$ -frame as  $\omega = [p \ q \ r]^T$ , the translational and rotational dynamics of the helicopter can be obtained as follows:

$$m\dot{V}_O = f_{air} + R_{OB}f_B + mg \quad (3)$$

$$\dot{R}_{OB} = R_{OB}\tilde{\omega} \quad (4)$$

$$J\dot{\omega} = -\tilde{\omega}J\omega + \tau \quad (5)$$

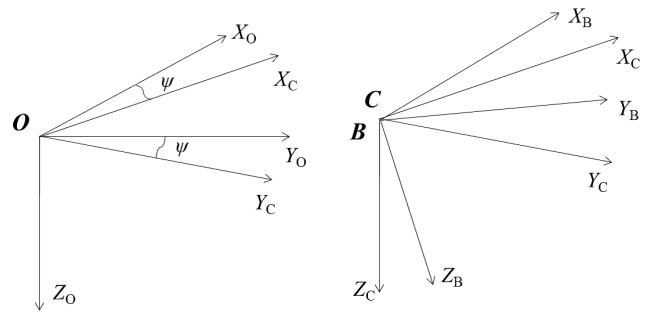


Fig. 3 Coordinate system.

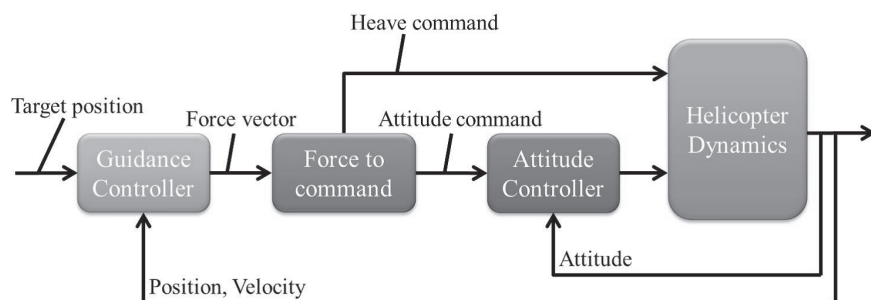


Fig. 2 Overview of entire control system.

Here,  $m$  is the mass of the helicopter,  $f_{air}$  is the aerodynamic resistance force,  $f_B$  is the external force generated by the main and tail rotors on  $B$ -frame, and  $g$  is the gravitational acceleration vector  $g = [0, 0, g]^T$ .  $J = \text{diag}(I_{xx}, I_{yy}, I_{zz})$  is an inertia matrix,  $\tau$  is the external torque vector impressed on the helicopter, and  $\tilde{\omega}$  is the skew-symmetric matrix that represents the vector product and defined as

$$\tilde{\omega} = \begin{bmatrix} 0 & -r & q \\ r & 0 & -p \\ -q & p & 0 \end{bmatrix} \quad (6)$$

The external force and torque are generated by the main and tail rotors and are obtained by

$$f_B = \begin{bmatrix} 0 \\ 0 \\ -T_m \end{bmatrix}, \quad \tau = \begin{bmatrix} hT_m \sin(b) + k_\beta b \\ hT_m \sin(a) + k_\beta a \\ l_x T_t \end{bmatrix} \quad (7)$$

Here,  $a$  and  $b$  are the flapping angles of the main rotor,  $T_m$  is the thrust of the main rotor,  $T_t$  is the thrust of the tail rotor, and  $k_\beta$  is the spring constant that expresses the stiffness of the rotor blade.  $l_x$  is the  $X_B$  axis component of the distance between the center of the tail rotor and the center of gravity, and  $h$  is the distance between the center of the main rotor and the center of gravity. Let the rudder control input be  $\delta_{rud}$  and the collective pitch control input be  $\delta_{col}$ ; then, the thrusts of the main and tail rotors are

$$T_m = K_{col}\delta_{col}, \quad T_t = K_{rud}\delta_{rud} - K_g r \quad (8)$$

The second equation in Eq. (8) includes the angular rate feedback by the rate gyro. Here,  $K_{col}$  and  $K_{rud}$  are appropriate coefficients and  $K_g$  is the feedback gain of the rate gyro. Finally, considering  $\delta_{ail}$  and  $\delta_{ele}$  as the aileron and elevator control inputs, respectively, and  $c$  and  $d$  as the flapping angles of the stabilizer bar, the first-order flapping equations of the main rotor and the stabilizer bar are [3]

$$\frac{16}{\gamma_b \Omega} \dot{a} = -a - \frac{16}{\gamma_b \Omega} \omega_y + K_{L3}c + K_{L1}\delta_{ele} \quad (9)$$

$$\frac{16}{\gamma_b \Omega} \dot{b} = -b - \frac{16}{\gamma_b \Omega} \omega_x + K_{L3}d + K_{L1}\delta_{ail} \quad (10)$$

$$\frac{16}{\gamma_s \Omega} \dot{c} = -c - \frac{16}{\gamma_s \Omega} \omega_y + K_{L2}\delta_{ele} \quad (11)$$

$$\frac{16}{\gamma_s \Omega} \dot{d} = -d - \frac{16}{\gamma_s \Omega} \omega_x + K_{L2}\delta_{ail} \quad (12)$$

Here,  $K_{L1}$ ,  $K_{L2}$ , and  $K_{L3}$  are constants related to the linkage mechanism of the helicopter.  $\gamma_b$  and  $\gamma_s$  are aerodynamic dimensionless numbers related to the main rotor and stabilizer bar called blade lock number, and  $\Omega$  expresses the angular velocity of the main rotor. Using Eqs. (3)–(12), and introducing the three-axis position on  $O$ -frame as  $X = [x \ y \ z]^T$ , the 16th-order full-state model of a small unmanned helicopter is as follows:

$$\dot{x}_f = f(x_f, u_f) \quad (13)$$

$$x_f = [x \ y \ z \ v_x \ v_y \ v_z \ \phi \ \theta \ \psi \ p \ q \ r \ a \ b \ c \ d]^T \quad (14)$$

$$u_f = [\delta_{ail} \ \delta_{ele} \ \delta_{rud} \ \delta_{col}]^T \quad (15)$$

Directly applying NMPC to this full-state model is difficult because the order of the model is so high, which makes it computationally expensive. Therefore, a simpler model for NMPC design is desired.

## 2.2 Attitude Control System

The attitude dynamics are extracted from the original full-state model of Eq. (13) for the design of attitude control system. To simplify the attitude model, we made the following assumptions.

- The roll and pitch angles of the helicopter are sufficiently small.
- The flapping angles of the main rotor and stabilizer bar are sufficiently small.
- The yaw rate is stabilized and almost equal to zero.

The first and second assumptions are required for the approximations as  $\sin(u) \simeq u$ ,  $\cos(u) \simeq 1$ , and ( $u = \phi, \theta, a, b$ ) and to decouple the attitude dynamics. These assumptions are easily satisfied in hovering or low speed situations. These hover or low speed assumption is valid for practical mission because most of the small unmanned helicopter are operated below 3 m/s in complicated environment where the collision likely occurs. The third assumption is required to decouple the dynamics of the angular velocity and can be achieved by using the local feedback of the rate gyro system. Under these assumptions, the following linear and decoupled attitude model can be extracted from the full-state model.

$$\begin{bmatrix} \dot{p} \\ \dot{\phi} \\ \dot{b} \\ \dot{d} \end{bmatrix} = \begin{bmatrix} 0 & 0 & \frac{hT_m + k_\beta}{I_{xx}} & 0 \\ 1 & 0 & 0 & 0 \\ -1 & 0 & \frac{-\gamma_b \Omega}{16} & \frac{\gamma_b \Omega}{16} K_{L3} \\ -1 & 0 & 0 & \frac{-\gamma_s \Omega}{16} \end{bmatrix} \begin{bmatrix} p \\ \phi \\ b \\ d \end{bmatrix} + \begin{bmatrix} 0 \\ 0 \\ \frac{\gamma_b \Omega}{16} K_{L1} \\ \frac{\gamma_s \Omega}{16} K_{L2} \end{bmatrix} \delta_{ail} \quad (16)$$

$$\begin{bmatrix} \dot{q} \\ \dot{\theta} \\ \dot{a} \\ \dot{c} \end{bmatrix} = \begin{bmatrix} 0 & 0 & \frac{hT_m + k_\beta}{I_{yy}} & 0 \\ 1 & 0 & 0 & 0 \\ -1 & 0 & \frac{-\gamma_b \Omega}{16} & \frac{\gamma_b \Omega}{16} K_{L3} \\ -1 & 0 & 0 & \frac{-\gamma_s \Omega}{16} \end{bmatrix} \begin{bmatrix} q \\ \theta \\ a \\ c \end{bmatrix} + \begin{bmatrix} 0 \\ 0 \\ \frac{\gamma_b \Omega}{16} K_{L1} \\ \frac{\gamma_s \Omega}{16} K_{L2} \end{bmatrix} \delta_{ele} \quad (17)$$

$$\begin{bmatrix} \dot{\psi} \\ \dot{r} \end{bmatrix} = \begin{bmatrix} 0 & 1 \\ 0 & -K_g \end{bmatrix} \begin{bmatrix} \psi \\ r \end{bmatrix} + \begin{bmatrix} 0 \\ K_{rud} \end{bmatrix} \delta_{rud} \quad (18)$$

Using the derived model, a linear quadratic integral controller was designed for the roll and pitch axes, and a simple PD controller was designed for the yaw axis. The flight experiment was carried out using the designed controller. The experimental results are shown in Fig. 4. The solid line represents the desired attitude, the dashed line represents the experimental result, and the chain line shows the simulation results using the derived model. The figure shows that the attitude of the helicopter can be stabilized and that it can follow the desired attitude. The simulation results correlated well with the experimental results. Therefore, the validity of the derived attitude model and efficiency of the designed controller were confirmed.

## 2.3 Guidance Control System

The guidance control system is designed using NMPC. If the attitude control system presented in the previous section is applied, the attitude of the helicopter can be assumed to immediately follow the desired attitude. Therefore, the attitude closed loop system could be virtually regarded as an actuator from the translational dynamics of the helicopter, and the dynamics of the attitude control system is regarded as the dynamics of the actuator. Then, the rotation matrix  $R_{OB}$  in Eq. (3) can

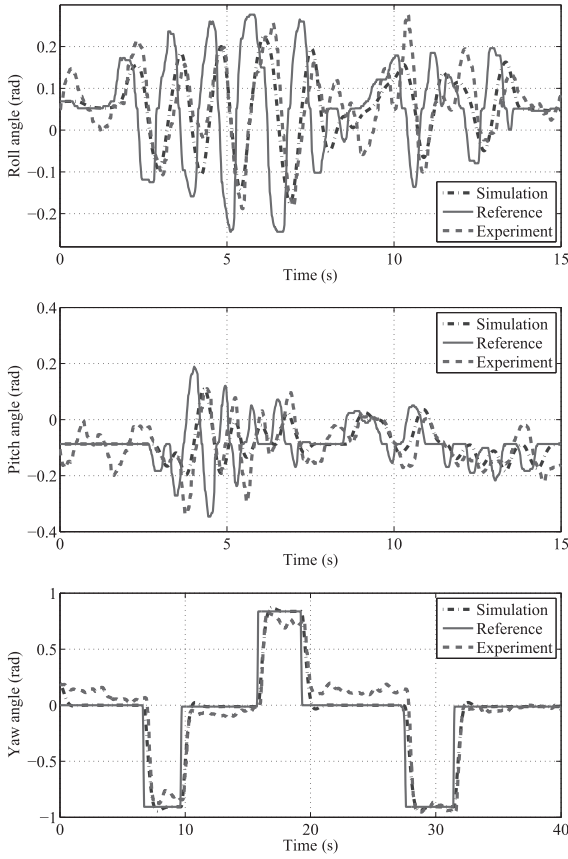


Fig. 4 Experimental result of attitude control.

be regarded as a virtual control input for the system.  $f_B$  is determined by the collective pitch input  $\delta_{col}$ . Thus, we can adopt the external force on  $O$ -frame  $f_O = R_{OB}f_B = [f_x, f_y, f_z]^T$  as the control input for the translational dynamics of the helicopter. Under these assumptions, the translational equation of motion on  $O$ -frame Eq. (3), can be simplified as follows:

$$\begin{aligned} m\dot{v}_x &= -k_x \dot{v}_x^2 + f_x \\ m\dot{v}_y &= -k_y \dot{v}_y^2 + f_y \\ m\dot{v}_z &= -k_z \dot{v}_z^2 + f_z + mg \end{aligned} \quad (19)$$

Here,  $k_x$ ,  $k_y$ , and  $k_z$  denote coefficients relate to aerodynamic resistance. Generally,  $k_x$ ,  $k_y$ , and  $k_z$  are proportional to the surface area of the object. When the helicopter is hovering,  $k_z$  can be considered as constant. However,  $k_x$  and  $k_y$  may vary in conjunction with the yaw angle because the helicopter shape is long in the anteroposterior direction (Fig. 5). Therefore,  $k_x$  and  $k_y$  are considered to be a function of  $\psi$ :

$$k_x(\psi) = k_{xy}(l_a + l_b \sin \psi), \quad k_y(\psi) = k_{xy}(l_a + l_b \cos \psi) \quad (20)$$

Considering Eq. (20) and  $\dot{x} = v_x$ ,  $\dot{y} = v_y$ , and  $\dot{z} = v_z$ , the nonlinear state space equation for translation is

$$\dot{\mathbf{x}}_t = \mathbf{f}_t(\mathbf{x}_t(t), \mathbf{u}_t(t)) \quad (21)$$

Here,  $\mathbf{f}_t$  is a nonlinear function, the state vector is  $\mathbf{x} = [x \ y \ z \ v_x \ v_y \ v_z]^T$ , and the input vector is  $\mathbf{u} = [f_x \ f_y \ f_z \ \psi]^T$ . The NPMC based guidance controller is designed using the model as follows.

For the NMPC design, a mathematical model of the helicopter and performance index used for optimization are needed.

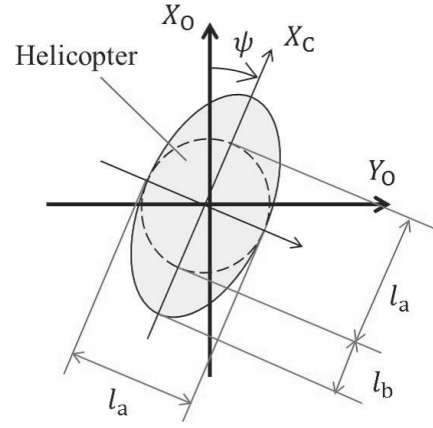


Fig. 5 Translational model.

The mathematical model is derived as Eq. (21); thus, the performance index is still needed. In this study, we adopted the following performance index.

$$\begin{aligned} J = \Phi(\bar{\mathbf{x}}_t(t+T)) &+ \int_t^{t+T} \{L(\bar{\mathbf{x}}_t(t+\tau), \bar{\mathbf{u}}_t(t+\tau)) \\ &+ \gamma_u P_u(\bar{\mathbf{u}}_t(t+\tau)) + \gamma_x P_x(\bar{\mathbf{x}}_t(t+\tau))\} d\tau \end{aligned} \quad (22)$$

$\bar{\mathbf{x}}_t$  and  $\bar{\mathbf{u}}_t$  are the estimated state and input as predicted by the model. On the right-hand side, the first and second terms are terminal cost and stage cost, respectively, and they are defined as follows:

$$\Phi(\bar{\mathbf{x}}_t(t+T)) = \bar{\mathbf{x}}_t^T(t+T) \mathbf{S} \bar{\mathbf{x}}_t(t+T) \quad (23)$$

$$L(\bar{\mathbf{x}}_t(\tau), \bar{\mathbf{u}}_t(\tau)) = \bar{\mathbf{x}}_t^T(\tau) \mathbf{Q} \bar{\mathbf{x}}_t(\tau) + \bar{\mathbf{u}}_t^T(\tau) \mathbf{R} \bar{\mathbf{u}}_t(\tau) \quad (24)$$

$\mathbf{S}$ ,  $\mathbf{Q}$ , and  $\mathbf{R}$  are weighting matrices. The third and fourth terms on the right-hand side of Eq. (22) are related to collision avoidance and input constraints.  $\gamma_u$  and  $\gamma_x$  are design parameters. The constraints are described in detail below.

The third term of Eq. (22) is related to input constraints. In the previous section, we assumed that the attitude of the helicopter is near the hovering state. Thus, the desired attitude angle should be limited to satisfy the assumption. We deal with such a limit as an inequality constraint:

$$g(\bar{\mathbf{u}}_t) = \bar{f}_x^2 + \bar{f}_y^2 - (mg \sin \alpha)^2 \leq 0 \quad (25)$$

Here, suffix  $i$  represents the  $i$ th estimate in the evaluation interval, and  $\alpha$  [rad] is the permissible maximum tilt angle of the helicopter. The relation between the external force and the tilt angle of the helicopter is shown in Fig. 6(a). We introduce such input constraints to the performance index as the penalty function  $P_u(\bar{\mathbf{u}}_t(t+\tau))$ , which can be obtained as

$$P_u(\bar{\mathbf{u}}_t) = \max\{0, g(\bar{\mathbf{u}}_t)\}^2. \quad (26)$$

The fourth term in Eq. (22) is the state constraints for collision avoidance. To avoid collision, a prohibited area is established around each helicopter or obstacle (Fig. 6(b)). The inequality constraints can be obtained as

$$g_x(\bar{\mathbf{x}}_t) = r^2 - \{(\bar{x}_t^i - x_a)^2 + (\bar{y}_t^i - y_a)^2\} \leq 0 \quad (27)$$

Here,  $r$  is the radius of the closed area. The penalty function related to the state constraint is obtained as follows:



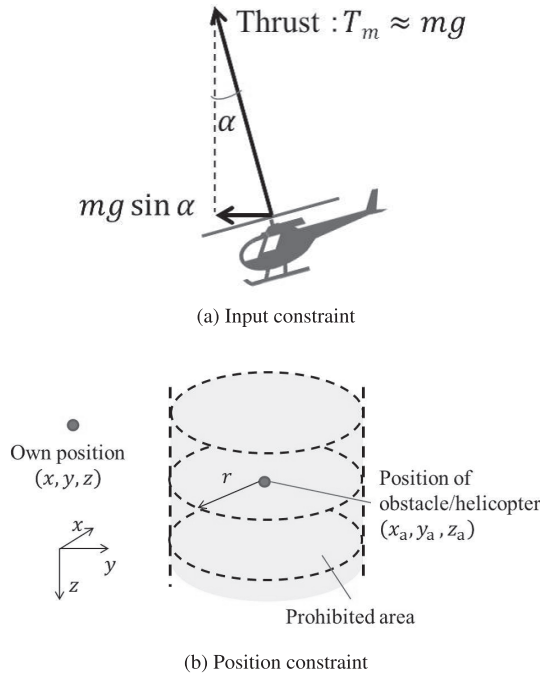


Fig. 6 Position and input constraints.

$$P_x(\bar{x}_t) = \max\{0, g(\bar{x}_t)\}^2 \quad (28)$$

Using the model Eq. (21) and performance index Eq. (22), the guidance control for a small helicopter with collision avoidance can be regarded as determining the optimal control to satisfy the following optimization problem.

$$\begin{aligned} & \text{Minimize : } J \\ & \text{Subject to : } \begin{cases} \dot{\bar{x}}_t(\tau) = f_t(\bar{x}_t(\tau), \bar{u}_t(\tau)) \\ \bar{x}_t(\tau)|_{\tau=0} = \mathbf{x}_t(t) \end{cases} \end{aligned} \quad (29)$$

Considering  $\lambda$  as the costate of the system, the stationary condition of the optimization problem can be obtained as follows:

$$\frac{\partial \mathbf{x}_t^*}{\partial \tau} = f(\mathbf{x}_t^*(t + \tau), \mathbf{u}_t^*(t + \tau)) \quad (30)$$

$$\mathbf{x}_t^*(\tau)|_{\tau=0} = \mathbf{x}_t(t) \quad (31)$$

$$\frac{\partial \lambda^*}{\partial \tau} = - \left( \frac{\partial H}{\partial \bar{x}_t} \right)^T (\mathbf{x}_t^*(t + \tau), \mathbf{u}_t^*(t + \tau), \lambda^*(t + \tau)) \quad (32)$$

$$\lambda^*(\tau)|_{\tau=T} = \left( \frac{\partial \Phi}{\partial \bar{x}_t} \right)^T (\mathbf{x}_t^*(T)) \quad (33)$$

$$\frac{\partial H}{\partial \bar{u}_t} (\mathbf{x}_t^*(t + \tau), \mathbf{u}_t^*(t + \tau), \lambda^*(t + \tau)) = 0 \quad (34)$$

Here, the symbol \* denotes the optimum solution, and  $H$  denotes the Hamiltonian, which is

$$H(\mathbf{x}, \mathbf{u}, \lambda) = L(\mathbf{x}, \mathbf{u}) + \gamma_x P_x(\mathbf{x}) + \gamma_u P_u(\mathbf{u}) + \lambda^T f \quad (35)$$

The optimal control series  $\mathbf{u}^*$  could be obtained by solving Eqs. (30)–(34), and we use the initial value of  $\mathbf{u}^*$  for the current control input to the system.

Finally, the desired attitude and rotor thrust are calculated by using the control input. First, the relation between the external force and the rotor thrust  $T_m$  is obtained as

$$\mathbf{f}_O = \begin{bmatrix} f_x \\ f_y \\ f_z \end{bmatrix} = \mathbf{R}_{OB} \begin{bmatrix} 0 \\ 0 \\ -T_m \end{bmatrix} \quad (36)$$

Table 1 Simulation parameters.

$S$	diag(1, 1, 1, 1, 1, 1)	$Q$	diag(1, 1, 1, 15, 15, 15)
$R$	diag(30, 30, 1, 10)	$\gamma_u$	100
$\gamma_x$	1	$r$	0.4 m
$\alpha$	5 deg		

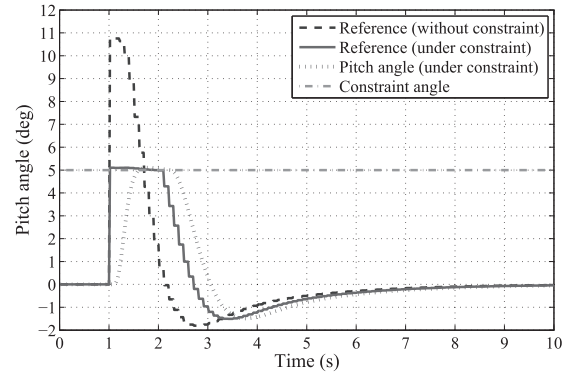


Fig. 7 Verification of input constraint.

From the equation,  $T_m$  can be obtained as

$$T_m = \|\mathbf{f}_O\| \quad (37)$$

Next, the basis for the  $\mathbf{Z}_B$  axis on  $\mathbf{O}$ -frame can be obtained as

$$\mathbf{z}_B = - \frac{\mathbf{f}_O}{\|\mathbf{f}_O\|} \quad (38)$$

because the rotor thrust is aligned with the negative direction of the  $\mathbf{Z}_B$  axis. The basis for the  $\mathbf{X}_C$  axis on  $\mathbf{O}$ -frame can be expressed by using yaw angle  $\psi$  as follows:

$$\mathbf{x}_C = [\cos \psi \quad \sin \psi \quad 0]^T \quad (39)$$

Using  $\mathbf{z}_B$  and  $\mathbf{x}_C$ , the bases for the  $\mathbf{Y}_B$  and  $\mathbf{X}_B$  axes are obtained as

$$\mathbf{y}_B = \frac{\mathbf{z}_B \times \mathbf{x}_C}{\|\mathbf{z}_B \times \mathbf{x}_C\|}, \quad \mathbf{x}_B = \mathbf{y}_B \times \mathbf{z}_B \quad (40)$$

Finally, the rotation matrix  $\mathbf{R}_{OB}$  can be calculated by using Eqs. (1), (38), and (40). Equation (2) and yaw angle  $\psi$  can be used to uniquely determine the attitude angles  $\phi$  and  $\theta$ .

### 3. Simulation

A numerical simulation was performed using the designed control system. The effectiveness of the designed state and input constraints was verified. We solved the two-point boundary-value problem of Eqs. (30)–(34) using the C/GMRES method [27]. The parameters and weighting matrices used in the simulation are listed in Table 1. The prediction step  $N$  was set to 20, the sampling time  $\Delta t$  and prediction interval  $\Delta \tau$  were each 0.1 s, and the prediction horizon  $T$  was  $T = N \times \Delta \tau = 2$  s.

#### 3.1 Verification of Input Constraint

First, the input constraint was verified. In this simulation, the position reference was set as the step signal, and the desired attitude generated by the guidance controller was compared for the cases with and without the input constraint. The result is shown in Fig. 7. The dashed line represents the desired attitude without the input constraint, the solid line is with the constraint, and the dotted line represents the attitude angle that follows the desired attitude with the constraint. The figure clearly shows that the desired attitude was kept to 5° when there was an input

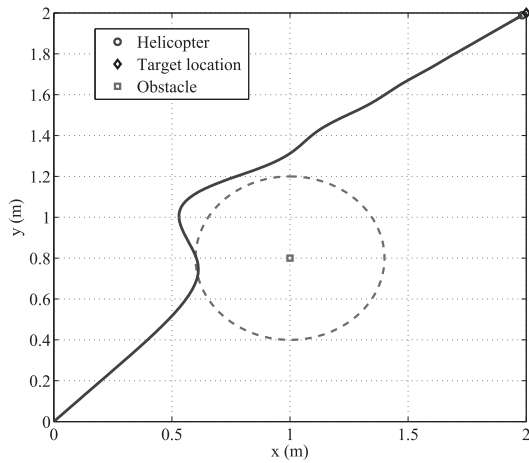


Fig. 8 Simulation result of collision avoidance.

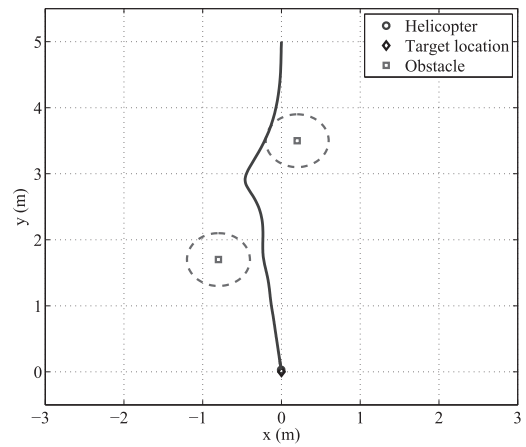
constraint, whereas a large overshoot appeared when there was no constraint. The attitude angle was also suppressed to below  $5^\circ$ , which indicates the effectiveness of the input constraint.

### 3.2 Verification of State Constraint

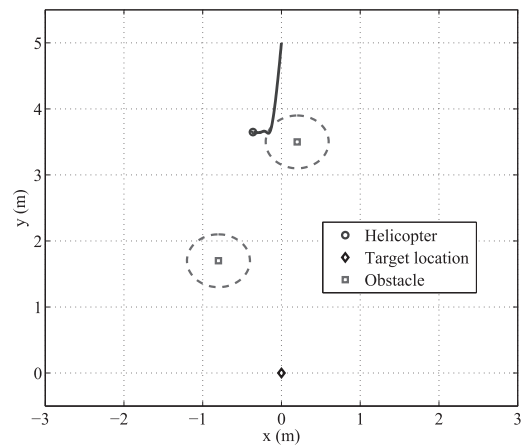
The state constraint for collision avoidance was verified. First, collision avoidance was simulated for a static obstacle. The result is shown in Fig. 8. The initial position of the helicopter was set to  $(0, 0, 0)$  on  $O$ -frame, and the target position was set to  $(2, 2, 0)$ . Then, the static obstacle was arranged at  $(1, 0.8, 0)$ . The figure shows that the helicopter avoided the no entry area and converged to the target position, so the state constraint for collision avoidance was shown to be effective.

Next, the collision avoidance was simulated for two static obstacles. In the simulation, two obstacles were arranged between the helicopter and target position. For comparison, the potential field method was also used for obstacle avoidance. The results are shown in Fig. 9: (a) NMPC and (b) potential field method. In the case of the potential field method, desired position of the helicopter is recursively updated based on the potential field, and NMPC without any state constraints is used to stabilize the helicopter on the desired position. Figure 9(a) shows that the helicopter was successfully guided to the target position without collision when the proposed guidance control system was used. In contrast, Fig. 9(b) shows that the helicopter stopped on the way because it fell into the local minima in the case of potential field method. Of course, the result depends on the design of the potential field. However, in the case of more complicated situation such as collision avoidance between multiple helicopters, it is difficult to ensure that the system has no local minima by using only uniform potential field. And, the larger the system is, the more complicated the design of potential field is. By contrast, it is easy to apply NMPC to the complicated case without change of the objective function. From the results, the superiority of the proposed guidance system was shown.

Finally, the proposed method was applied to the collision avoidance of two helicopters. In the simulation, two helicopters flew intersecting trajectories using NMPC. The result is shown in Fig. 10. Collision avoidance was achieved using the proposed method. Thus, the results show that the proposed guidance system can be easily applied to the collision-free guidance control of multiple small helicopters.



(a) NMPC



(b) Potential field method

Fig. 9 Collision avoidance for two obstacles.

## 4. Experiment

A flight experiment was carried out using the designed guidance control system. An overview of the experimental setup is shown in Fig. 11. The optical motion capture system and inertial measurement unit (IMU) were used for control. The IMU used sent the data to PC by Bluetooth. In the PC, the states of the helicopter (position, velocity, and attitude) were estimated using the extended kalman filter (EKF) and used for control calculation. Finally, the control inputs calculated by the guidance and attitude controller were sent to the helicopter by a wireless transmitter. A guidance control experiment for collision avoidance of a static obstacle was performed to establish the efficiency of the designed guidance controller. The implementation environment and control parameters are listed in Table 2. In the experiment, the prediction step  $N$  was set to 20, the sampling time  $\Delta t$  and prediction interval  $\Delta \tau$  were each 0.1 s, and prediction horizon  $T$  is  $T = N \times \Delta \tau = 2$  s. The average calculation time of NMPC was 5.8 ms, which was shorter than the sampling time. The initial position of the helicopter was set to  $(-1.2, -1.2, -0.5)$  on  $O$ -frame and regulated to the origin. The obstacle was at  $(-0.6, -0.6, 0)$  and the radius of no the entry area was set to 0.4 m. The result is shown in Fig. 12. For comparison, the same control experiment was performed using NMPC without a state constraint. In the figure, the solid line

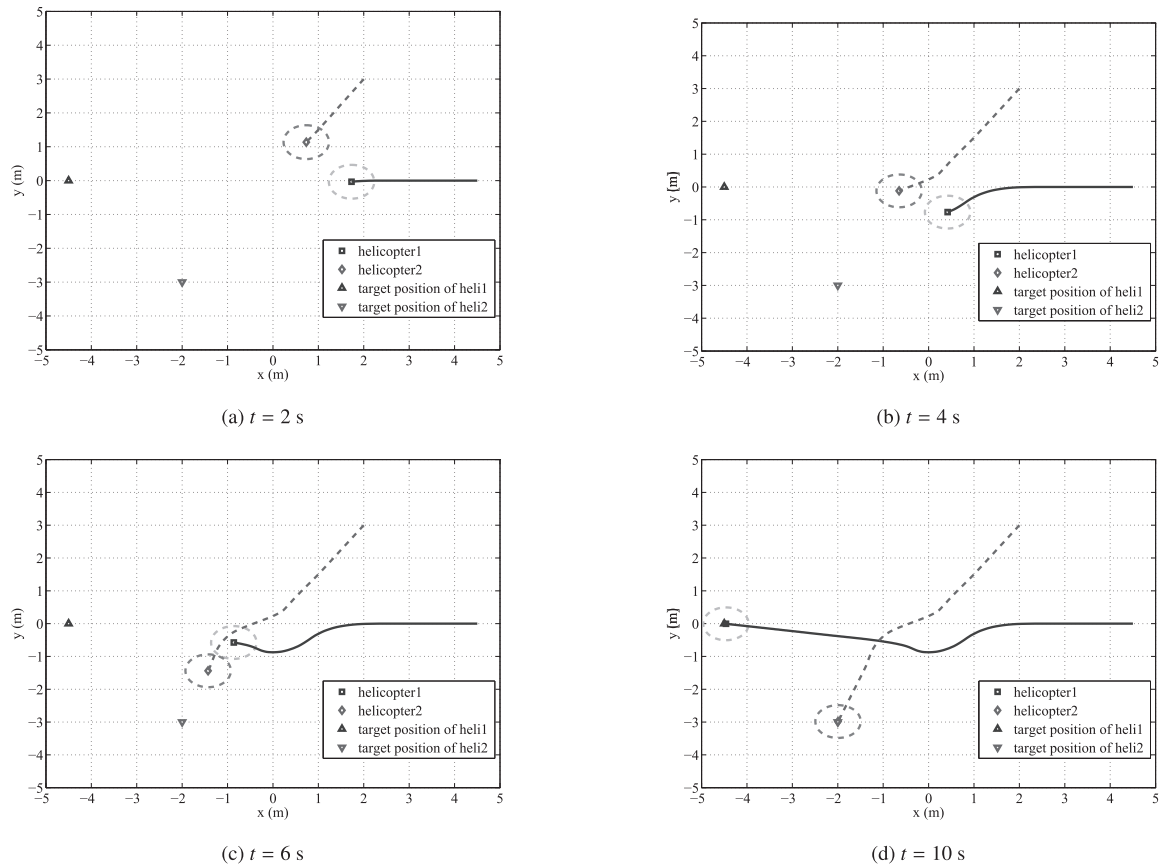


Fig. 10 Simulation result of collision avoidance of two helicopters.

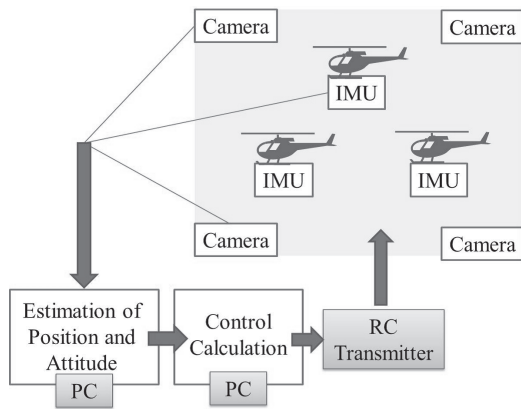


Fig. 11 Experimental setup.

Table 2 Control environment and parameters.

Environment	
CPU	Intel Core2 Duo
Memory	3.45 GB
Language	C++
Parameters	
$S$	$\text{diag}(60, 60, 200, 500, 500, 10)$
$Q$	$\text{diag}(20, 20, 5, 2, 2, 2)$
$R$	$\text{diag}(200, 200, 200, 200)$
$\gamma_x$	3000
$\gamma_u$	10000

represents the flight trajectory of the helicopter with collision avoidance, and the chain line represents the trajectory without collision avoidance. The helicopter went straight to the origin and passed near the obstacle when the control system without

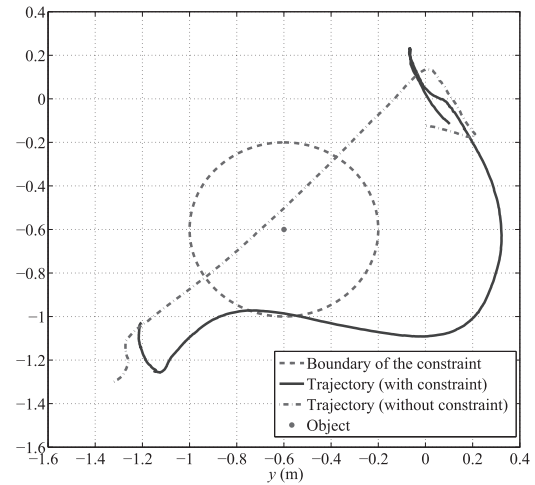


Fig. 12 Experimental result.

the state constraint was used. In contrast, the helicopter avoided the obstacle and converged to the origin when the controller was used with the state constraint. Thus, collision-free guidance control of a small unmanned helicopter was achieved using the proposed guidance control system based on NMPC. However, there are some differences between the result of the simulation Fig. 8 and experiment Fig. 12. And also the weighting matrices of each case is different. These differences seems to be caused by aerodynamic damping of main rotor which is not included in Eqs. (9), (10), and (20).

## 5. Conclusion

The authors designed a collision-free guidance control system for small unmanned helicopters. NMPC was used in the guidance controller to avoid collision. A hierarchical control structure consisting of an attitude control system and guidance control system was adopted for the control system. A simple nonlinear translational model of the helicopter was proposed to reduce the computational cost of NMPC. The effectiveness of the proposed collision-free guidance control system was verified by a numerical simulation and flight experiment.

In future work, NMPC considering inner loop dynamics will be designed to improve the performance of the guidance control and will realize the simultaneous flight of multiple small unmanned helicopters.

## Acknowledgments

This work was partly supported by JSPS KAKENHI Grant Number 24760185.

## References

- [1] C.K. Oh and G.J. Barlow: Autonomous controller design for unmanned aerial vehicles using multi-object genetic programming, *Proceedings of Congress on Evolutionary Computation 2004*, Vol. 2, pp. 1538–1545, 2004.
- [2] J.M. Eklund, J. Sprinkle, and S. Sastry: Implementing and testing a nonlinear model predictive tracking controller for aerial pursuit/evasion games on a fixed wing aircraft, *Proceedings of 2005 American Control Conference*, Vol. 3, pp. 1509–1514, 2005.
- [3] B. Mettler: System identification modeling of a small-scale unmanned rotorcraft for flight control design, *Journal of American Helicopter Society*, Vol. 47, No. 1, pp. 50–63, 2002.
- [4] H.J. Kim and D.H. Shim: A flight control system for aerial robots: Algorithm and experiment, *Journal of Control Engineering Practice*, Vol. 11, No. 12, pp. 1389–1400, 2003.
- [5] N.J. Eric, K.K. Suresh, and K. Kannan: Adaptive trajectory control for autonomous helicopters, *AIAA Journal of Guidance Control and Dynamics*, Vol. 28, No. 3, pp. 524–538, 2005.
- [6] C.L. Castillo, W. Alvis, M. Castillo-Effen, W. Moreno, and K. Valavanis: Small unmanned helicopter simplified and decentralized optimization-based controller design for non-aggressive flights, *International Journal on Systems Science and Applications*, Vol. 1, No. 3, pp. 303–315, 2006.
- [7] S. Shen, N. Michael, and V. Kumar: Autonomous multi-floor indoor navigation with a computationally constrained MAV, *Proceedings of IEEE International Conference on Robotics and Automation 2011*, pp. 20–25, 2011.
- [8] J.H. Lee, B.M. Min, and E.T. Kim: Autopilot design of tilt-rotor UAV using particle swarm optimization method, *Proceedings of the 2007 International Conference of Control, Automation and Systems*, pp. 1629–1633, 2007.
- [9] H. Stone and K.C. Wong: Preliminary design of a tandem-wing tail-sitter UAV using multi-disciplinary design optimization, *Proceedings of International Aerospace Congress*, pp. 707–720, 1997.
- [10] S.J. Lee, S.P. Kim, T.S. Kim, H.K. Kim, and H.C. Lee: Development of autonomous flight control system for 50 m unmanned airship, *Proceedings of 2004 Intelligent Sensors, Sensor Networks Information Processing Conference*, pp. 457–461, 1997.
- [11] N. Michael, D. Mellinger, Q. Lindsey, and V. Kumar: The GRASP multiple micro UAV testbed, *IEEE Robotics and Automation Magazine*, Vol. 17, Issue 3, pp. 56–65, 2010.
- [12] D.H. Shim, H.J. Kim, and S. Sastry: Decentralized nonlinear model predictive control of multiple flying robots, *Proceedings of 42nd IEEE Conference on Decision and Control*, 2003, Vol. 4, pp. 3621–3626, 2003.
- [13] N. Michael, J. Fink, and V. Kumar: Cooperative manipulation and transportation with aerial robots, *Autonomous Robots*, Vol. 30, Issue 1, pp. 73–86, 2011.
- [14] O. Khatib: Real-time obstacle avoidance for manipulators and mobile robots, *International Journal of Robotics Research*, Vol. 5, No. 1, pp. 90–98, 1986.
- [15] A.A. Kandil, A. Wagner, A. Gotta, and E. Badreddin: Collision avoidance in a recursive nested behaviour control structure for Unmanned Aerial Vehicles, *Proceedings of IEEE International Conference on Systems Man and Cybernetics (SMC) 2010*, pp. 4276–4281, 2010.
- [16] A. Patel and S. Winberg: UAV collision avoidance: A specific acceleration matching control approach, *Proceedings of IEEE AFRICON, 2011*, pp. 1–6, 2011.
- [17] J.-W. Park, H.-D. Oh, and M.-J. Tahk: UAV collision avoidance based on geometric approach, *Proceedings of SICE Annual Conference 2008*, pp. 2122–2126, 2008.
- [18] F. Morteza and N. Homayoun: An unscented model predictive control approach to the formation control of nonholonomic mobile robots, *Proceedings of IEEE International Conference on Robotics and Automation 2012*, pp. 1576–1582, 2012.
- [19] Y. Chai, S. Wei, M. Guo, and R. Ling: Distributed model predictive control with communication complete failure for multi-aircrafts formation, *Proceedings of Chinese Control and Decision Conference 2009*, pp. 4663–4668, 2009.
- [20] A. Richards and J. How: Decentralized model predictive control of cooperating UAVs, *43rd IEEE Conference on Decision and Control*, 2004, CDC, Vol. 4, pp. 4286–4291, 2004.
- [21] Y. Kuwata, A. Richards, T. Schouwenaars, and J.P. How: Distributed robust receding horizon control for multivehicle guidance, *IEEE Transactions on Control Systems Technology*, Vol. 15, No. 4, pp. 627–641, 2007.
- [22] K. Kon, S. Habasaki, H. Fukushima, and F. Matsuno: Model predictive based multi-vehicle formation control with collision avoidance and localization uncertainty, *2012 IEEE/SICE International Symposium on System Integration (SII)*, pp. 212–217, 2012.
- [23] J. Shin and H.J. Kim: Nonlinear model predictive formation flight, *IEEE Transactions on Systems, Man and Cybernetics, Part A: Systems and Humans*, Vol. 39, No. 5, pp. 1116–1125, 2009.
- [24] D. Alejo, R. Conde, J.A. Cobano, and A. Ollero: Multi-UAV collision avoidance with separation assurance under uncertainties, *IEEE International Conference on Mechatronics, 2009, ICM 2009*, pp. 1–6, 2009.
- [25] A. Bemporad and C. Rocchi: Decentralized linear time-varying model predictive control of a formation of unmanned aerial vehicles, *2011 50th IEEE Conference on Decision and Control and European Control Conference (CDC-ECC)*, pp. 7488–7493, 2011.
- [26] D. Lee, H. Lim, and H.J. Kim: Obstacle avoidance using image-based visual servoing integrated with nonlinear model predictive control, *2011 50th IEEE Conference on Decision and Control and European Control Conference (CDC-ECC)*, pp. 5689–5694, 2011.
- [27] T. Ohtsuka: A continuation/GMRES method for fast computation of nonlinear receding horizon control, *Automatica*, Vol. 40, Issue 4, pp. 563–574, 2004.



=====

**Satoshi SUZUKI (Member)**



He received his M.E. and Ph.D. (Eng.) degrees from Chiba University, Japan, in 2006 and 2008, respectively. In 2009, he joined Shinshu University, where he is currently an Assistant Professor of the Faculty of Textile Science and Technology. His research interests include control of autonomous vehicle. He is a member of JSME, IEEE, and RSJ.

**Takahiro ISHII**



He received his B.E. and M.E. degrees from Shinshu University, Japan, in 2011 and 2013, respectively. He is currently a mechanical engineer of Yamaha Motor.

**Yoshihiko AIDA**



He received his B.E. degree from Shinshu University, Japan, in 2012. He is currently an M.E. student at Shinshu University. His research interests include control system design for multiple vehicles.

**Yohei FUJISAWA**



He received his B.E. degree from Shinshu University, Japan, in 2013. He is currently an M.E. student at Shinshu University. His research interests include control of small unmanned helicopter.

**Kojiro IZUKA**



He received his B.E. and M.E. degrees from Tokyo University of Agriculture and Technology, Japan, in 1997 and 1999, respectively, and Ph.D. (Eng.) degree from The Graduate University for Advanced Studies (SOKENDAI), Japan, in 2006. He joined Shinshu University in 2008, where he is currently an Associate Professor of Interdisciplinary Graduate School of Science Technology. His research interests include development of an exploration rover for lunar and planet surface with rough terrain. He is a member of JSME, RSJ and IEEE.

**Takashi KAWAMURA (Member)**



He received his B.E., M.E., and Ph.D. (Eng.) degrees from The University of Electro-Communications, Japan, in 1987, 1989, and 1992, respectively. He joined Shinshu University in 1992, where he is currently an Associate Professor of Interdisciplinary Graduate School of Science Technology. His research interests include intelligent and skillful robot system. He is a member of JSME, IEEE and JSKE.

=====